Acta Oceanol. Sin., 2019, Vol. 38, No. 3, P. 159–165
https://doi.org/10.1007/s13131-019-1408-4
http://www.hyxb.org.cn
E-mail: hyxbe@263.net

A hydrothermal investigation system for the *Qianlong-II* autonomous underwater vehicle

Tao Wu[1]*, Chunhui Tao[1, 2], Jinhui Zhang[1], Ao Wang[3], Guoyin Zhang[1], Jianping Zhou[1], Xianming Deng[1]

[1] Key Laboratory of Submarine Geosciences, Second Institute of Oceanography, Ministry of Natural Resources, Hangzhou 310012, China

[2] School of Oceanography, Shanghai Jiaotong University, Shanghai 200030, China

[3] Institute of Geophysics and Geomatics, China University of Geosciences, Wuhan 430074, China

Received 3 February 2018; accepted 20 March 2018

Abstract

Qianlong-II is a fully autonomous underwater vehicle designed for the investigation of submarine resources, particularly polymetallic sulfides. It was used to successfully explore hydrothermal fields on the Southwest Indian Ridge. Here, we summarized the exploration of hydrothermal systems using *Qianlong-II*, including detailed descriptions of its implementation along with the systems used for data management and fast mapping. We also introduced a method to remove platform magnetic interference using magnetic data while *Qianlong-II* is spinning. Based on hydrothermal anomalies collected by *Qianlong-II*, we developed a rapid method for locating hydrothermal vents. Taking one dive as an example, we systemically demonstrated the process for analyzing hydrothermal survey data to locate hydrothermal vents.

Key words: *Qianlong-II*, autonomous underwater vehicle, data management, hydrothermal investigation

Citation: Wu Tao, Tao Chunhui, Zhang Jinhui, Wang Ao, Zhang Guoyin, Zhou Jianping, Deng Xianming. 2019. A hydrothermal investigation system for the *Qianlong-II* autonomous underwater vehicle. Acta Oceanologica Sinica, 38(3): 159–165, doi: 10.1007/s13131-019-1408-4

1 Introduction

With the development of seafloor survey platforms, more and more researchers are focusing on hydrothermal field study. The first hydrothermal chimney was found at 21°N in the East Pacific Rise on April 21, 1979 by the human-occupied vehicle, *Alvin* (Corliss et al., 1979). Since then, plentiful seafloor hydrothermal activities have been found in intensive environments such as mid-ocean ridges, back-arc basins, and intraplate volcanic centers (Rona et al., 1993; Fouquet et al., 1997; Herzig, 1999; Edmonds and German, 2004; Tao et al., 2007).

Hydrothermal investigation has special significance as the unique ecosystems near hydrothermal vents contain abundant genetic resources and may even provide clues to the origin of life (Baross and Hoffman, 1985; Martin et al., 2008). Polymetallic sulfides, products of the interaction between heat, bedrock, and seawater in hydrothermal fields, are considered a submarine resource with broad exploitative prospects found in polymetallic nodules and cobalt-rich crusts (Galley et al., 2007). Hydrothermal sulfides exposed on the seafloor are being mined, allowing researchers to visually study the ore-forming mechanism of polymetallic sulfides. Furthermore, hydrothermal fluids constitute a main source of leakage of materials and heat in the deep earth (Johnson and Pruis, 2003).

However, the spatial distribution and dimensions of mineralized bodies are limited because of the characteristics of hydrothermal sulfide mineralization. Their geophysical signatures are limited to hundreds or even dozens of meters (Tivey and Dyment, 2010). Also, their hydrothermal anomalies are only distinct within hundreds of meters above the seafloor (Thomson et al., 1995), thus they can only be detected using near-bottom surveys. Developments in near-bottom geophysical surveying, including remote-operated vehicles (ROV), human occupied vehicles (HOV), and autonomous underwater vehicles (AUV), have enabled researchers to investigate hydrothermal sulfides.

Surveys of seabed mineral resources conducted using AUVs, such as the Remote Environmental Monitoring Unit System (REMUS) (Allen et al., 1997; Purcell et al., 2002; Shcherbina et al., 2008), the *Autonomous Benthic Explorer* (*ABE*) (German et al., 2008), and *Sentry* (Yoerger et al., 2006; Jakuba et al., 2011), which were carried out by Woods Hole Oceanographic Institute. The *R* series of AUVs, led by the University of Tokyo, made outstanding contributions to Japanese oceanographic research, particularly through investigations of oceanic ridges and submarine volcanoes (Ura et al., 2001, 2004, 2007).The *Autosub* AUV in England (Millard et al., 2003) and the *Hugin* series of AUVs in Norway (Vestgard et al., 1999; Hagen, 2001) have also been successfully used to investigate marine resources.

In China, AUV research began in the 1980s. The AUVs *Explorer*, *CR-01*, and *CR-02*, along with the *Qianlong* AUV series, were developed in succession (Liu et al., 2002; Wu et al., 2014). The newest AUV in the *Qianlong* series, *Qianlong-II*, is a deep-sea investigation system that specializes in exploring deep-sea

Foundation item: The Technology Upgrading and Scientific Applications of the 4 500 m Depth Rated Qianlong II AUV under contract No. 2017YFC0306803; the National Key R&D Program of China under contract No. 2018YFC0309901; the COMRA Major Project under contract Nos DY135-S1-01-06 and DY135-S1-01-01.
*Corresponding author, E-mail: wutao1988@126.com

mineral resources. It successfully explored hydrothermal vent fields on the Southwest Indian Ridge (SWIR). Here we provide a detailed description of the investigation, data management, and fast mapping systems that *Qianlong-II* uses to perform the hydrothermal investigation.

2 Overview of the investigation system on the *Qianlong-II*

2.1 *Carrying of equipment*

Qianlong-II, which is shown in Fig. 1, is the platform for scientific sensors and has a highly intelligent control system, excellent maneuverability, and high-precision positioning and navigation. The main specifications of *Qianlong-II* are shown in Table 1. The functions of *Qianlong-II* include spinning, obstacle avoidance, and navigation with contour altitude or depth, allowing it to accommodate deep-sea hydrothermal surveying, even in complex terrain. *Qianlong-II* is equipped with a standard suite of control and scientific sensors. The control sensors include a piezometer, a Doppler velocity logger (DVL), an attitude sensor, a PHINS inertial navigation sensor, and forward-looking sonar. *Qianlong-II* was designed to explore deep-sea resources, particularly hydrothermal sulfides. Therefore, scientific sensors consist of geophysical sensors such as a multi-beam sonar system, a bathymetric sidescan sonar system (BSSS), a three-component magnetometer, and oceanographic sensors made up of a CTD, multi-parameter water probe meters, an oxidation-reduction potential (ORP) sensor and a methane sensor. Some of the above sensors are identified in Fig. 1.

Before conducting hydrothermal investigations using *Qianlong-II*, sensor reliability should be ensured via calibration or testing, and a magnetic diurnal station should be set up to collect data and rectify daily measurement variations throughout the operation. Before each dive, the methane sensor should be preheated for hours or even several days if the sensor has been unused for a long time. When operating depth is reached, the AUV should be allowed to spin and collect magnetic data to correct for tri-axial magnetometer interference caused by the AUV. It is worth mentioning that the AUV should maintained at a depth of 5–10 m above the seafloor if there are plans to photograph the seafloor to obtain substrate information.

2.2 *Navigation method*

Acoustic navigation is an important and effective positioning method for underwater platforms and should be aided by long-baseline (LBL), short-baseline (SBL), or ultrashort-baseline (USBL) acoustic systems (Bellingham et al., 1994). Preparation of the LBL system is time-consuming, but its positioning accuracy is high. SBL and USBL systems, which are conventional equipment on ships, are small and comparatively convenient to position. *Qianlong-II* uses a combination of a DVL (WHN 300 kHz), an inertial navigation system (INS; PHINS 6000: https://www.ixblue.com/products/phins-6000), and an LBL system for positioning (Mu et al., 2013). If the required navigation accuracy is not too high, the LBL system can be replaced with a USBL system.

Here, we provide an introduction to the aforementioned navigation methods. For the LBL system, at least three transponders should be moored on the seafloor to communicate with the transmitter and receiver of the RAMSES 6000 the LBL system (https://www.ixblue.com/sites/default/files/downloads/ixblue-ps-

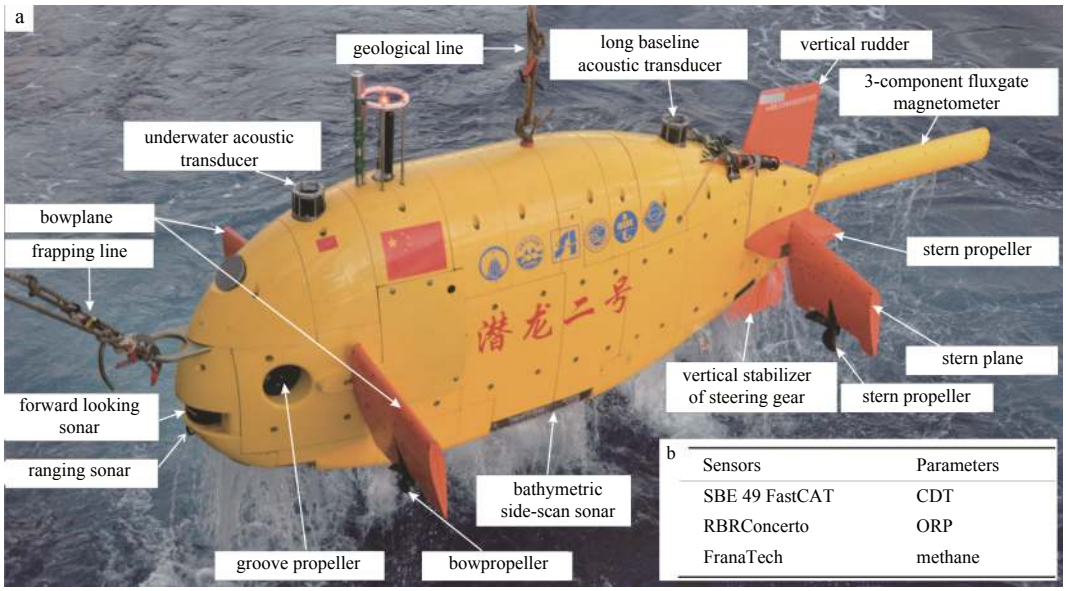

Fig. 1. Photograph of the *Qianlong-II* as it arrives at the sea surface. a. Main control and scientific sensors, and b. sensors.

Table 1. Specifications of the *Qianlong-II*

Specifications	Parameter indexes
Dimensions	length = 3.46 m; width = 0.71 m; height = 1.3 m
Weight	≤1 100 kg
Maximum operating depths	4 500 m
Navigational speed	cruising speed of 2 kn, maximum speed of 3 kn
Descent/ascent rates (unpowered)	down 35 m/min; up 43 m/min
Endurance	≥ cruise 30 h (at cruising speed of 1 m/s)
Available energy	lithium-ion batteries (~23 kWh)

ramses-02-2014-web.pdf) on the AUV (Baccou and Jouvencel, 2002). The PHINS 6000 periodically sends an acoustic signal and receives responses from the transponders in order to determine and adjust its position while performing the AUV navigation in the water. Further, it is worth mentioning that the positions of the transponders are located by a USBL system on the mothership by letting the mothership run laps. A series of positions are measured for each transponder, and the center of these positions is obtained by the least-squares method, which is regarded as the transponder's position.

The positioning accuracy of the LBL system is high, with a relative error of <0.1 m; however, absolute error is incurred because the transponders are located using a USBL system. Absolute error (Δd) is a product of the positioning accuracy (p) of the USBL system and the target depth (h) (Eq. (1)). The value of p can assess letting mothership navigate around "8" track line (IXSEA, 2004), and it relates to opening angle (α), which is the arctan function of the radius (r) of the "8" track line and h (Eq. (2)). The value of p for the USBL system on *Xiangyanghong10*, *Qianlong-II*'s mothership, is 2‰, 2.7‰ and 6.1‰ when α is 30°, 60° and 120°, respectively. For example, its accuracy is approximately 4 m when α=30° and h=2 000 m.

$$\Delta d = ph, \tag{1}$$

$$\alpha = 2\arctan(r/h). \tag{2}$$

We attempted to use the USBL system along with the LBL system for navigation and positioning while investigating hydrothermal sulfides on the SWIR using *Qianlong-II*. This system no requires time to moor and measure transponders. Furthermore, INS of PHINS can autonomously navigate as planned, if technology is mature, the mothership could carry out other investigation near area. We conducted a successful near-shore test; however, the technique is far from mature and suffers from drift error and accumulation of error with time.

3 The hydrothermal investigation system of *Qianlong-II*

Previously, hydrothermal exploration relied upon deep-tow instruments equipped with sensors that could locate sites of active hydrothermal vent, but the locking length scales are relatively larger range than hydrothermal area with only hundreds (even only dozens) of meters. However, AUV has high-precision positioning and navigation that benefits from an intelligent control system, inertial navigation system, and LBL or USBL system for positioning, and the accuracy of positioning can be determined to few meters. *Qianlong-II*, which is similar to *ABE* (German et al., 2008), *Sentry* (Yoerger et al., 2006; Jakuba et al., 2011), *R* series AUV (Ura et al., 2001, 2004, 2007), etc., performs a variety of conventional and unconventional surveys including sonar surveys, hydrothermal plume surveys, and near-bottom magnetic and photo surveys. Here, we have depicted a hydrothermal investigation system of *Qianlong-II* that contains data management, rapid mapping, and anomaly positioning and near-bottom magnetic data correction systems. Further, we observe that this method of magnetic correction is an innovative method.

3.1 *Data management system*

The control system, navigation system, and survey system of *Qianlong-II* are relatively independent, and survey information has corresponding physical meaning until matches location, depth, altitude, etc. The data management system, which is shown in Fig. 2a, was developed to improve efficiency. The data management system can record sensor data, including photographs, BSSS documents, and custom files; preprocess and standardize data (e.g., delete erroneous data, transform methane data with hexadecimal to decimal, and convert electric potential information from the magnetometer to magnetic induction); integrate all sensor data together, and match data with corresponding vehicle information (e.g., location, depth, altitude and cruising speed) by time series. Using the data management system, the integrated data can allow to review, statistics and select, and it can be exported document directly according to requirement. Moreover, the system can be used to record, manage and query information related to the voyage, equipment, port and crew.

3.2 *Rapid mapping and anomaly positioning*

A three-phase method was employed to locate and map hydrothermal vent sites by *ABE* (Yoerger et al., 2007). Phase 1 involved a loosely spaced (~250 m) grid survey in the nonbuoyant

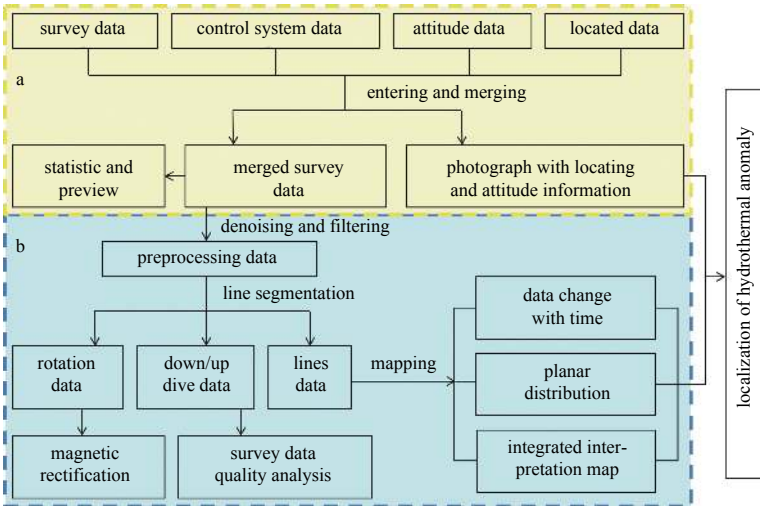

Fig. 2. The management system and process procedure for hydrothermal exploration with *Qianlong-II*. a. Data management system, and b. the rapid post-processing software for hydrothermal exploration. a and b together form the rapid system for identifying the locations of hydrothermal vents.

plume layer (~100–200 m) with the goal of finding the most intense hydrothermal anomalies. In Phase 2, the AUV surveyed 50 m above the seafloor with track lines spaced 30 m apart to intercept rising plume stems while making detailed bathymetric and magnetic field maps of the seafloor. Based on these results, a Phase 3 survey was conducted 5–10 m above the seafloor, during which detailed electronic photographs were produced, which could be combined to make photo-mosaics and determine seafloor characteristics. Referencing to the previous patterns, we developed rapid post-processing software in order to perform hydrothermal investigation. This software can rapidly map and localize anomalies in order to plan the AUV's next missions.

Figure 2b shows software function and process procedure. With integrated data, the software can remove noise and filter data and classify track-lines as dive, horizontal circle, survey lines, and floating, for processing and analyzing. The software can also automatically and quickly map changing curves with time, planar distribution, and integrated anomaly of each parameter with survey line data. Using the software, we can analyze the depth curve of survey data while AUV moves down and up and compare the consistency of the junction points data, with the same/similar position and different time, which extracted from cross-line and survey lines.

In addition, we developed a rapid system for identifying the locations of hydrothermal vents using comprehensive hydrochemical anomalies and geological interpretation based on photographs. To infer hydrothermal anomalies, we plot survey data on the same time axis, set reasonable thresholds for each parameter (including methane concentration, turbidity and oxidation reduction potential (ORP)), and consider a possible hydrothermal anomaly if one or more parameters exceed the threshold. Meanwhile, we show planar distribution of each survey data and callout near-bottom photos if have in corresponding area. Combining these maps, we can analyze whether a true hydrothermal anomaly exists and delineate it if it does.

3.3 *High-precision, near-bottom magnetic data*

Qianlong-II contains a three-component magnetometer. Data collected by this instrument can be used to determine the geomagnetic structure of the hydrothermal area and to study inactive hydrothermal sulfide areas (Caratori et al., 2012; Tivey and Dyment, 2010). However, the magnetometer is prone to magnetic disturbances from the surrounding environment (e.g., ferromagnetic materials and strong electric currents from the platform and carried equipment). Effective magnetic anomalies can only be obtained after correcting for magnetic interference. Wu et al. (2018) systematically studied the choice of magnetometer location on the platform and methods of magnetic correction. Using a probe extension pole, they placed the magnetometer far away from batteries, motors, and other sources of interference. The tri-axial magnetometer interference caused by the AUV can be corrected by allowing AUV to rotate horizontally. Here, we suggest a method to allow AUV to hover and rotate instead of circling around a small radius (about 10 m) to obtain AUV spinning data during the *Qianlong-II* survey of hydrothermal sulfides on the SWIR. This would reduce *Qianlong-II* circling time and achieve a good correction result (Fig. 3). Furthermore, as our research area on the SWIR is far away from constant geomagnetic observatories, we moored a magnetometer over the seafloor as a temporary geomagnetic station and obtained magnetic changes up to 200 nT in a day, and the diurnal variation was more than the expected variation within 40–60 nT. Thus, it is necessary to consider and reduce daily magnetic variation. The reason for this phenomenon needs further study.

4 Application example

Following a series of experimental tests on land, in a lake, and at sea, *Qianlong-II* obtained hydrothermal anomalies and near-bottom magnetic data in a hydrothermal sulfide area on the SWIR from January to March in 2016. The hydrothermal investigation system is useful for the analysis of hydrothermal survey data and the location of hydrothermal vents. Taking the AUV029 dive as an example, we illustrate the analysis procedure using the investigation system.

After the diving mission was completed and *Qianlong-II* was withdrawn to the deck, survey data, control system data, navigation data, and altitude data were obtained from the system. Further, data were successively entered, and erroneous data (e.g., wrong identifier, broken text field) were automatically checked and deleted by the data management system. This allowed us to obtain an integrated document with a common data format after formatting and merging the data that was entered by the system. Opening the document directly in the software that was used for rapid mapping and anomaly positioning depicted the tracking map and the time and depth curves of the survey data. As depicted in Fig. 4, we intercept moving down/up data from time-depth curve (Fig. 4b), cut survey lines data from track line (Fig. 4a), and obtain horizontal circle data from time-heading curve (Fig. 4d).

Based on the data that were obtained when the AUV moved down and up, we analyzed the dependability of some survey data

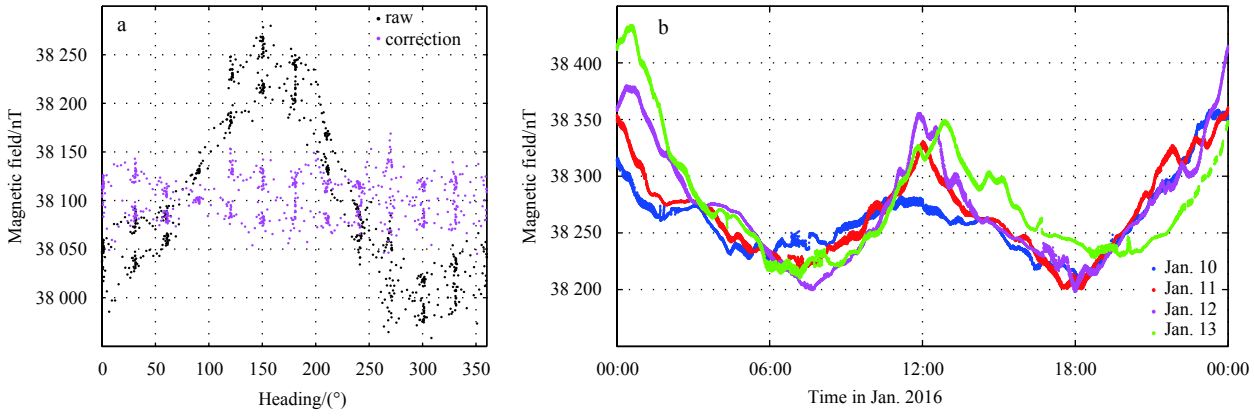

Fig. 3. Correction results of the AUV heading interference with spinning data (a), and magnetic diurnal observation in the research area during AUV work (b).

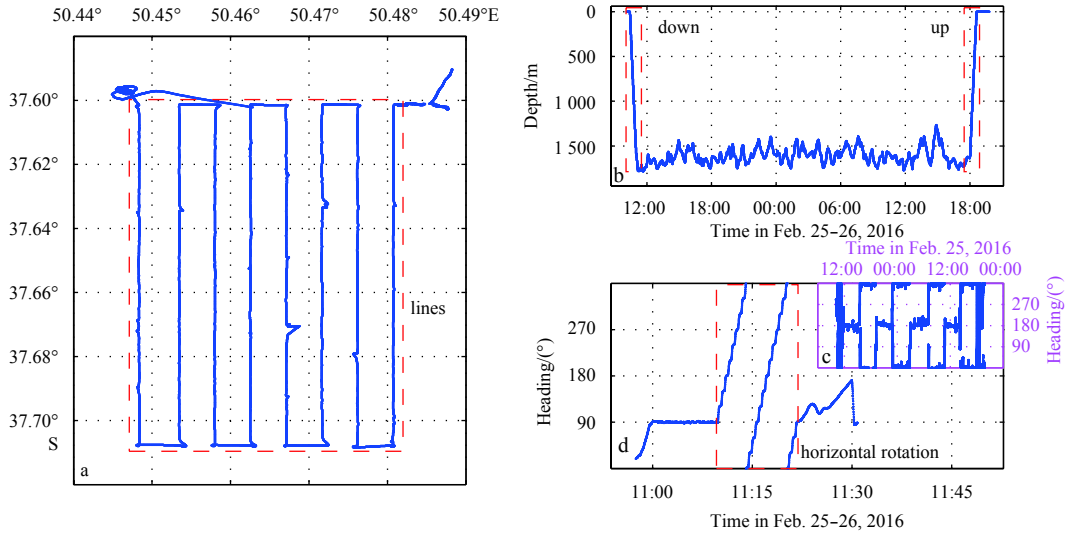

Fig. 4. Tracking map (a), time-depth curve (b), and time-heading curve of the AUV029 dive (c, d). d is the magnified time-heading curve while AUV spinning and is part curve of c.

with values closely associated with depth. Figure 5 shows the depth curves for different CTD measurement parameters, including temperature, conductivity, salinity, and velocity, as the AUV changed depth. Each of the measurement results of diving down data is in concordance with the floating up at the same depth. The data of methane concentration, turbidity, and ORP exhibit no direct relation to depth; however, they are effective in order to compare the data on survey lines along with the background.

We plotted these parameters on the same time axis to verify the presence of hydrothermal anomalies. Accoording to the principle, if more than one parameter exhibits an anomaly during the same period, we could infer existence of a hydrothermal anomaly. ORP, turbidity and methane are present and depict an obvious anomaly at approximately 17:30, 21:10 and 00:30, respect-

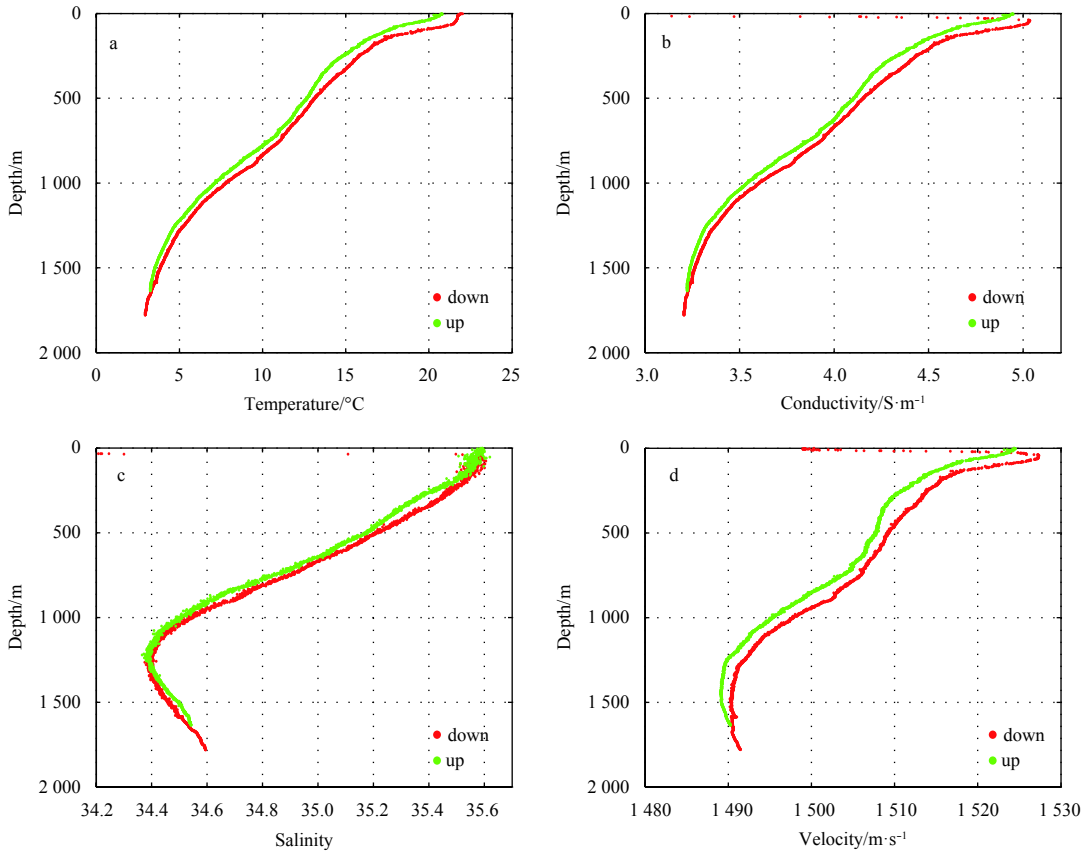

Fig. 5. Depth curves of CTD parameters while the AUV changed depth during the AUV029 dive. a, b, c and d are temperature-, conductivity-, salinity- and velocity-depth curves, respectively.

ively, as depicted in Fig. 6. Therefore, it is almost certain that there are hydrothermal anomalies above the known hydrothermal area. Without any doubt the location and range of the corresponding anomaly could be delineated using their planar distribution, however, we intend to depict their corresponding results as figures and to systematically expand and interpret the hydrothermal and magnetic anomalies in our future publications. Besides, existing survey data also indicated an obvious hydrothermal anomaly, and sulfide samples were obtained from the anomalous area (Tao et al., 2014). We obtained near-bottom photos and presented hydrothermal bioglyphs and sulfides in the anomalous area during the AUV020 dive (Fig. 7).

5 Conclusion

Qianlong-II is a deep-sea investigation system specially designed for the investigation of deep-sea mineral resources. It has been successfully used to explore hydrothermal fields on the SWIR. *Qianlong-II* is able to obtain high-resolution micro-geomorphology data, data on hydrothermal anomalies in the water column, and near-bottom magnetic information, and has an effective system for collecting, processing, and analyzing survey data. During the operation of *Qianlong-II*, we identified a series of problems that need to be addressed. For example, we could supply more room and a standby interface for detection systems and study and select the suitable carrying patterns (integration or combination) according to the investigation task. We should also strengthen the AUVs autonomy, such as, real-time replanning survey lines, or taking photos (AUV should descend 5–10 m up to sea-bottom) over hydrothermal anomaly area. To achieve real autonomy and independent judgment of hydrothermal anomalies, we should collect and accumulate data on the properties of water column anomalies in different types of hydrothermal areas

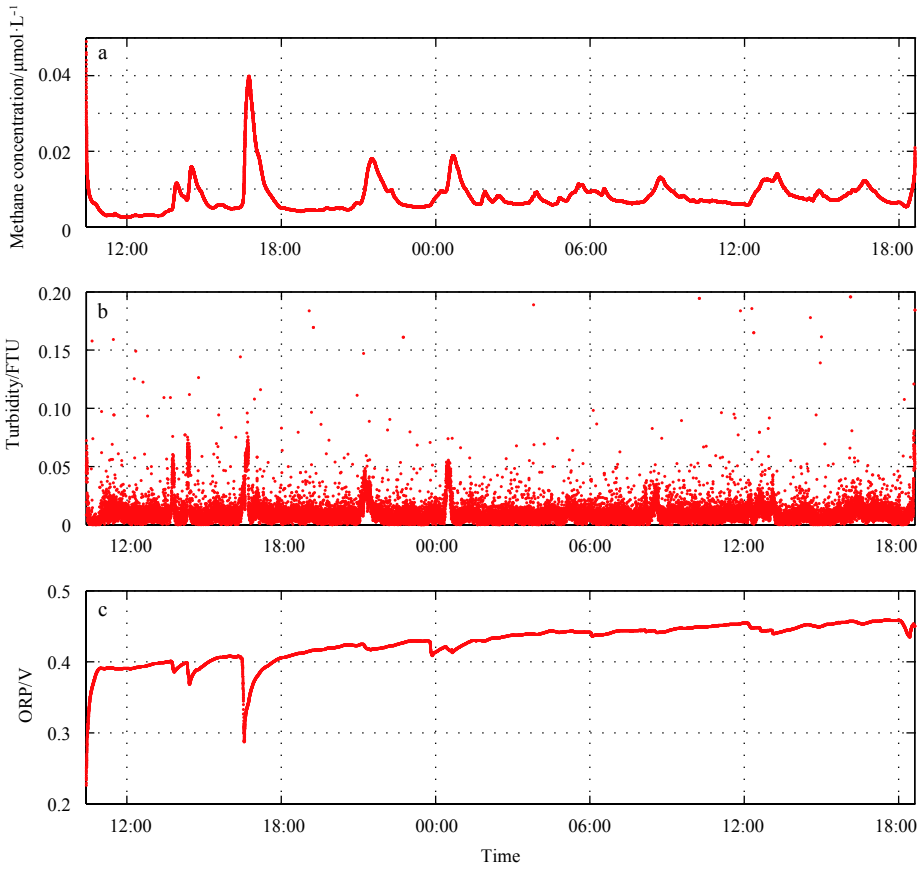

Fig. 6. Integrated hydrothermal anomalies vs. time during the AUV029 dive. a. Methane concentration, b. turbidity, and c. ORP.

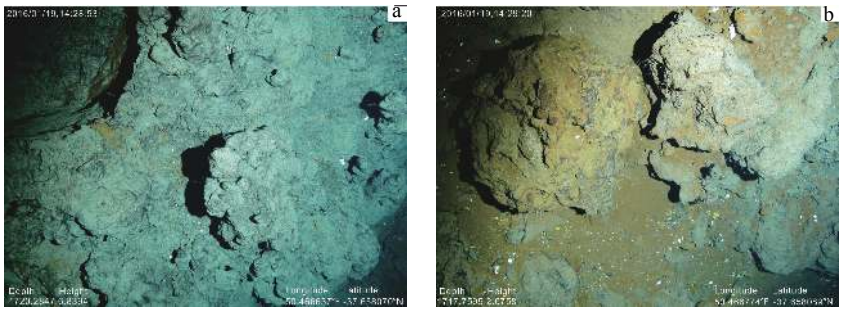

Fig. 7. Photographs of hydrothermal sulfides and bioglyphs taken during the AUV020 dive. a. Suspected sulfide chimney, and b. massive sulfide (yellow color) and relics of mussels (white color).

and improve the real-time capabilities to merge, process, and interpret survey data. These improvements will be considered when updating *Qianlong-II* and when developing the next generation of AUVs.

Acknowledgements

We thank the experimental team members of the 4 500 m *Qianlong-II* AUV technology application system.

References

Allen B, Stokey R, Austin T, et al. 1997. REMUS: a small, low cost AUV; system description, field trials and performance results. In: MTS/IEEE Conference Proceedings Oceans. Halifax, NS, Canada: IEEE, 2: 994–1000

Baccou P, Jouvencel B. 2002. Homing and navigation using one transponder for AUV, postprocessing comparisons results with long base-line navigation. In: Proceedings of 2002 IEEE International Conference on Robotics and Automation. Washington, DC, USA: IEEE, 4004–4009

Baross J A, Hoffman S E. 1985. Submarine hydrothermal vents and associated gradient environments as sites for the origin and evolution of life. Origins of Life and Evolution of the Biosphere, 15(4): 327–345, doi: 10.1007/BF01808177

Bellingham J G, Goudey C A, Consi T R, et al. 1994. A second generation survey AUV. In: Proceedings of IEEE Symposium on Autonomous Underwater Vehicle Technology. Cambridge, MA, USA: IEEE, 148–155

Caratori T F, De Ronde C E J, Yoerger D, et al. 2012. 3-D focused inversion of near-seafloor magnetic data with application to the Brothers volcano hydrothermal system, Southern Pacific Ocean, New Zealand. Journal of Geophysical Research: Solid Earth, 117(B10): B10102

Corliss J B, Dymond J, Gordon L I, et al. 1979. Submarine thermal sprirngs on the galápagos rift. Science, 203(4385): 1073–1083, doi: 10.1126/science.203.4385.1073

Edmonds H N, German C R. 2004. Particle geochemistry in the Rainbow hydrothermal plume, Mid-Atlantic Ridge. Geochimica et Cosmochimica Acta, 68(4): 759–772, doi: 10.1016/S0016-7037(03)00498-8

Fouquet Y. 1997. Where are the large hydrothermal sulphide deposits in the oceans?. Philosophical Transactions of the royal Society A: Mathematical, Physical and Engineering Sciences, 355(1723): 427–441, doi: 10.1098/rsta.1997.0015

Galley A G, Hannington M D, Jonasson I R. 2007. Mineral deposits of Canada: A synthesis of major deposit types, district metallogeny, the evolution of geological provinces and exploration methods. Mineral Deposits Division, Special Publication, 5: 509–531

German C R, Yoerger D R, Jakuba M, et al. 2008. Hydrothermal exploration with the *Autonomous Benthic Explorer*. Deep Sea Research Part I: Oceanographic Research Papers, 55(2): 203–219, doi: 10.1016/j.dsr.2007.11.004

Hagen P E. 2001. AUV/UUV mission planning and real time control with the HUGIN operator system. In: Conference Proceedings MTS/IEEE Oceans 2001. Honolulu, HI, USA: IEEE, 1: 468–473

Herzig P M. 1999. Economic potential of sea-floor massive sulphide deposits: ancient and modern. Philosophical Transactions of the Royal Society A: Mathematical, Physical and Engineering Sciences, 357(1753): 861–875, doi: 10.1098/rsta.1999.0355

IXSEA. 2004. USBL Posidonia 6000 Positioning System, User's Manual . Brest, France.

Jakuba M V, Kinsey J C, Yoerger D R, et al. 2011. Exploration of the gulf of Mexico oil spill with the *sentry* autonomous underwater vehicle. In: Proceedings of the International Conference on Intelligent Robots and Systems (IROS) Workshop on Robotics for Environmental Monitoring (WREM)

Johnson H P, Pruis M J. 2003. Fluxes of fluid and heat from the oceanic crustal reservoir. Earth and Planetary Science Letters, 216(4): 565–574, doi: 10.1016/S0012-821X(03)00545-4

Liu Tao, Xu Qi'nan, WANG Huizheng, et al. 2002. "CR-02" 6000m AUV hull structure systems. Journal of Ship Mechanics, 6(6): 114–119

Martin W, Baross J, Kelley D, et al. 2008. Hydrothermal vents and the origin of life. Nature Reviews Microbiology, 6(11): 805–814, doi: 10.1038/nrmicro1991

Millard N W, McPhail S D, Stevenson P, et al. 2003. Multidisciplinary ocean science applications of an AUV: the Autosub science missions programme. In: Griffiths G, ed. The Technology and Applications of Autonomous Underwater Vehicles. Abingdon, UK: Taylor & Francis

Mu Lingji, Chen E, Huang Shenwei, et al. 2013. Mechatronic system design for science/work class ROV. Applied Mechanics and Materials, 284–287: 1867–1871

Purcell M, Alt C V, Allen B, et al. 2002. New capabilities of the REMUS autonomous underwater vehicle. In: Conference Proceedings OCEANS 2000 MTS/IEEE Conference and Exhibition. Providence, RI, USA: IEEE, 1: 147–151

Rona P A, Hannington M D, Raman C V, et al. 1993. Active and relict sea-floor hydrothermal mineralization at the TAG hydrothermal field, mid-Atlantic ridge. Economic Geology, 88(8): 1989–1989, doi: 10.2113/gsecongeo.88.8.1989

Shcherbina A Y, Gawarkiewicz G G, Linder C A, et al. 2008. Mapping bathymetric and hydrographic features of Glover's Reef, Belize, with a REMUS autonomous underwater vehicle. Limnology & Oceanography, 53(5part2): 2264–2272

Tao Chunhui, Lin Jian, Guo Shiqin. 2007. Discovery of the first active hydrothermal vent field at the ultraslowspreading Southwest Indian Ridge. InterRidge News, 16: 25–26

Tao Chunhui, Li Huaiming, Jin Xiaobing, et al. 2014. Seafloor hydrothermal activity and polymetallic sulfide exploration on the southwest Indian ridge. Chinese Science Bulletin, 59(19): 2266–2276, doi: 10.1007/s11434-014-0182-0

Thomson R E, Davis E E, Burd B J. 1995. Hydrothermal venting and geothermal heating in Cascadia Basin. Journal of Geophysical Research: Solid Earth, 100(B4): 6121–6141, doi: 10.1029/95JB00030

Tivey M A, Dyment J. 2010. The magnetic signature of hydrothermal systems in slow spreading environments. In: Rona P A, ed. Diversity of Hydrothermal Systems on Slow Spreading Ocean Ridges. Washington, DC: American Geophysical Union, 43–66

Ura T, Obara T, Nagahashi K, et al. 2004. Introduction to an AUV "r2D4" and its Kuroshima knoll survey mission. In: Oceans'04 MTS/IEEE Techno-Ocean'04. Kobe, Japan: IEEE, 2: 840–845

Ura T, Obara T, Takagawa S, et al. 2001. Exploration of Teisi Knoll by autonomous underwater vehicle "R-One robot". In: Conference Proceedings MTS/IEEE Oceans 2001. An Ocean Odyssey. Honolulu, HI, USA: IEEE, 1: 456–461

Ura T, Tamaki K, Asada A, et al. 2007. Dives of AUV "r2D4" to rift valley of central Indian mid-ocean ridge system. In: OCEANS 2007-Europe. Aberdeen, UK: IEEE, 1–6

Vestgard K, Storkersen N, Sortland J. 1999. Seabed surveying with the Hugin AUV. In: Proceedings of the 11th International Symposium on Unmanned Untethered Submersible Technology. Durham, New-Hampshire, USA: University of New Hampshire-marine Systems, 63–74

Wu T, Tao C H, Liu C, et al. 2018. Correction of tri-axial magnetometer interference caused by an autonomous underwater vehicle near-bottom platform. Ocean Engineering, 160(2018): 68–77

Wu Jianguo, Liu Jian, Xu Huixi. 2014. A variable buoyancy system and a recovery system developed for a deep-sea AUV Qianlong I. In: OCEANS 2014-TAIPEI. Taipei, Taiwan: IEEE, 1–4

Yoerger D R, Bradley A M, Jakuba M, et al. 2007. Autonomous and remotely operated vehicle technology for hydrothermal vent discovery, exploration, and sampling. Oceanography, 20(1): 152–161, doi: 10.5670/oceanog

Yoerger D R , Bradley A M , Martin S C , et al. 2006. The Sentry Autonomous Underwater Vehicle: Field Trial Results and Future Capabilities. In: AGU Fall Meeting Abstracts